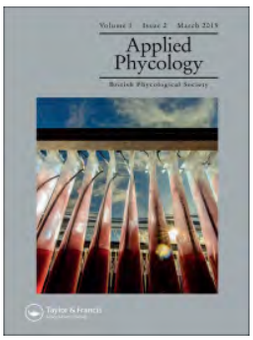

Applied Phycology

ISSN: (Print) (Online) Journal homepage: https://www.tandfonline.com/loi/tapy20

Characterization of vanadium-dependent bromoperoxidases involved in the production of brominated sesquiterpenes by the red alga *Laurencia okamurae*

Takafumi Ishikawa, Kenji Washio, Kensuke Kaneko, Xiao Rong Tang, Masaaki Morikawa & Tatsufumi Okino

To cite this article: Takafumi Ishikawa, Kenji Washio, Kensuke Kaneko, Xiao Rong Tang, Masaaki Morikawa & Tatsufumi Okino (2022) Characterization of vanadium-dependent bromoperoxidases involved in the production of brominated sesquiterpenes by the red alga *Laurencia okamurae*, Applied Phycology, 3:1, 120-131, DOI: 10.1080/26388081.2022.2081933

To link to this article: https://doi.org/10.1080/26388081.2022.2081933

APPLIED PHYCOLOGY
2022, VOL. 3, NO. 1, 120–131
https://doi.org/10.1080/26388081.2022.2081933

British Phycological Society
Understanding and using algae
Taylor & Francis
Taylor & Francis Group

Characterization of vanadium-dependent bromoperoxidases involved in the production of brominated sesquiterpenes by the red alga *Laurencia okamurae*

Takafumi Ishikawa[a], Kenji Washio[b], Kensuke Kaneko[c], Xiao Rong Tang[a], Masaaki Morikawa[b] and Tatsufumi Okino[a]

[a]Division of Environmental Science Development, Graduate School of Environmental Science, Hokkaido University, Kita-ku, Japan; [b]Division of Biosphere Science, Graduate School of Environmental Science, Hokkaido University, Kita-ku, Japan; [c]Material and Biological Engineering Course, National Institute of Technology, Hachinohe College, Tamonoki-aza, Japan

ABSTRACT

The red algal genus *Laurencia* produces abundant brominated metabolites, including cuparane- and laurane-type brominated sesquiterpenes. In order to gain insights into the biosynthesis mechanisms for brominated compounds, we focused on the vanadium-dependent bromoperoxidase (V-BPO). Four members of the homologous genes encoding for V-BPO were obtained from *L. okamurae* by PCR amplification. The recombinant V-BPO protein produced in *Escherichia coli* exhibited a significant brominating activity to monochlorodimedone. The function of V-BPO was examined by an assay using nerolidol as a relevant natural substrate. The enzyme properties of V-BPO were compared with those of related halogenating enzymes. The results indicate that V-BPO is one of the key enzymes responsible for the production of brominated compounds in *Laurencia*.

ARTICLE HISTORY
Received 25 June 2021
Accepted 14 May 2022

KEYWORDS
Brominated compound; bromoperoxidase; glutamine-rich repeat; *Laurencia*; red algae; Rhodophyta; sesquiterpene

Introduction

Laurencia is a genus of marine macroalgae in the Rhodophyta (class Florideophyceae, order Ceramiales and family Rhodomelaceae) and has 161 indexed species taxonomically accepted in AlgaeBase in January 2022 (Guiry & Guiry, 2022). *Laurencia* species are distributed on tropical to temperate shores all over the world. Previous studies have revealed that *Laurencia* is a rich producer of secondary metabolites with different chemical skeletons, including sesquiterpene, diterpene, triterpene and nonterpenoid C15-acetogenin. 512 sesquiterpenoids and 133 diterpenenoids of diverse structures have been identified in the genus (Harizani, Ioannou, & Roussis, 2016). Many of these products are halogenated due to the availability of chloride and bromide ions in seawater. It is noteworthy that bromide is frequently used by *Laurencia* for the synthesis of secondary metabolites, despite the fact that seawater contains a much higher concentration of chloride (559 mM) than bromide (0.86 mM).

The enzyme group of haloperoxidases is known to incorporate halogens into the organic molecules (Agarwal et al., 2017). Several types of haloperoxidases have been discovered in marine organisms, including Fe-haem haloperoxidase, vanadium haloperoxidase and non-haem haloperoxidase, among which vanadium-dependent bromoperoxidase (V-BPO) is the major class observed in the marine algae (EC 1.11.1.18) (Wever, Krenn, & Renirie, 2018). V-BPO accommodates vanadate (VO_4^{3-}) as an oxidizing agent at the metal centre and catalyses the oxidation of bromide utilizing hydrogen peroxide as a co-substrate. The resulting electrophilic bromonium cation (Br^+) attacks hydrocarbons and forms brominated products. Enzymatic bromination of the deduced precursors of natural products has been determined, using the commercially available lactoperoxidase (Ishihara, Kanoh, & Murai, 1995) and the purified enzyme from *Laurencia nipponica* (Fukuzawa et al., 1994). We have previously cloned the cDNAs for the V-BPO-like protein from *L. nipponica* and shown that the recombinant V-BPO protein simultaneously catalysed the bromination and cyclization of laurediol, a predicted precursor of C15-acetogenin (Kaneko et al., 2014). *L. nipponica* is likely to possess distinct members of V-BPO, including LnVBPO1 and LnVBPO2; however, the mechanisms leading to the prolific production of brominated compounds in *Laurencia* remain to be elucidated.

CONTACT Kenji Washio washi@ees.hokudai.ac.jp
Supplemental data for this article can be accessed online at https://doi.org/10.1080/26388081.2022.2081933

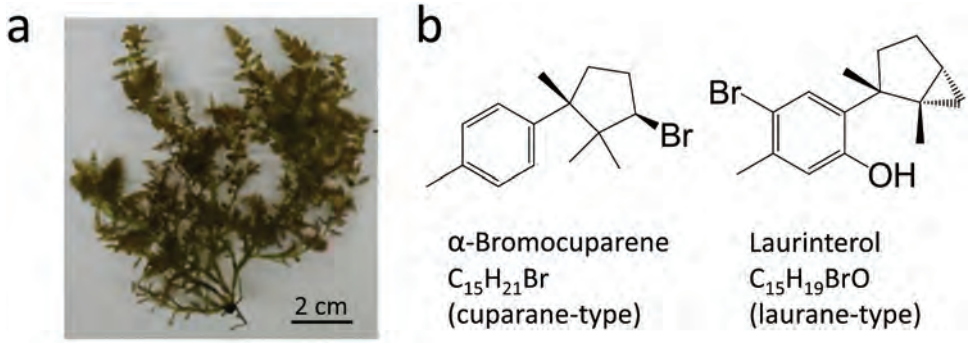

Figure 1. *Laurencia okamurae*. (a) The algal material of *L. okamurae* collected from Oshoro Bay. (b) Chemical structures of brominated sesquiterpenes α-bromocuparene and laurinterol produced by *L. okamurae*.

To understand the diverse biogenesis of brominated compounds, we focused on another species of *Laurencia*. *Laurencia okamurae* grows from subtropical to cold temperate regions of the Northwestern Pacific (Masuda, Abe, Suzuki, & Suzuki, 1996; Saito, 1989). Crossing tests using cultured strains indicated that *L. okamurae* is reproductively incompatible with *L. nipponica* (Abe & Masuda, 1998). The major secondary metabolites produced by the two species differ considerably. *L. okamurae* is known to synthesize a set of cuparane- and laurane-type sesquiterpenoids (Fig 1). *L. nipponica* mainly produces C15 acetogenins in addition to several chamigrene-type sesquiterpenoids, whereas cyclolaurane-type sesquiterpenoids have never been detected in *L. nipponica* (Harizani et al., 2016). The biosynthesis of sesquiterpenes starts from the intermediate precursor of C15 farnesyl pyrophosphate (FPP), where the coordination with terpene synthases and V-BPO appears to invoke the formation of initial scaffolds (Butler & Carter-Franklin, 2004). Terpene synthases have been recently reviewed in the red alga *Laurencia pacifica* (Kersten et al., 2017). We report here the identification and characterization of V-BPO from *L. okamurae* (LoVBPO).

Materials and methods

Cloning of the genes for LoVBPO

The *L. okamurae* material was collected from Oshoro-Bay (Otaru, Hokkaido) at the Sea of Japan in July 2012 and kept frozen until use (Fig 1). Genomic DNA was isolated from frozen samples of *L. okamurae* using a DNA isolation kit (Qiagen, Venlo, the Netherlands). Total RNA was prepared from the frozen samples by the RNeasy Midi Kit (Qiagen), and cDNAs were synthesized using the high-capacity cDNA reverse transcription kit (Thermo Fisher Scientific, Waltham, Massachusetts, USA). The homologous PCR primers were prepared according to published information for the red algal V-BPOs (Supplementary table S1). The PCR reactions were performed with the KOD plus DNA polymerase (Toyobo, Osaka, Japan). After the dA-overhang reaction by 10× A-attachment mix (Toyobo), the PCR products were excised after agarose gel electrophoresis, purified with the DNA extraction kit (Qiagen) and cloned into the pGEM-T easy vector (Promega, Madison, MD). The plasmid DNA was transformed into *Escherichia coli* DH5α and purified with the plasmid isolation kit. DNA sequencing used the BigDye terminator cycle sequencing on an ABI model 3100 DNA sequencer (Thermo Fisher Scientific). The LoVBPO genes without introns were verified by comparison of the nucleotide sequences between the genome PCR and the RT-PCR products (Supplementary fig. S1). To avoid the misread of PCR errors, more than five independent clones were selected for DNA sequencing.

To determine the entire nucleotide sequence of a coding region, adjacent regions of the gene for LoVBPO were obtained by inverse PCR (Sambrook & Russell, 2001). Genomic DNA was digested with the restriction enzyme *Nhe*I and self-ligated by the standard method. The self-ligated DNA was used for inverse PCR with two sets of the PCR primers complementary to the internal sequences of the coding region. The nucleotide sequences were determined by the chromosome walking technique. The sequence data have been submitted to the DDBJ database under the accession numbers LoVBPO1a (LC574879), LoVBPO1b (LC574880), LoVBPO2a (LC574877) and LoVBPO2b (LC574878).

Phylogeny and protein structure analysis

The amino acid sequences of V-BPOs were subjected to phylogenetic analysis using MAFFT (Katoh, Rozewicki, & Yamada, 2019; Kuraku, Zmasek, Nishimura, & Katoh,

2013) and FigTree (http://tree.bio.ed.ac.uk/software/figtree/). The monomer structure of V-BPO was predicted by SWISS-MODEL. The information on V-BPO from the red alga *Corallina officinalis* for which the X-ray crystal structure had been previously determined at a 2.2 Å resolution (Isupov et al., 2000) was utilized as a template for the structure prediction. The predicted model was visualized by PyMOL (The PyMOL Molecular Graphics System, Version 2.4, Schrödinger, LLC).

Preparation of the recombinant protein

The pET21a vector (Merck KGaA, Darmstadt, Germany) was used for the overproduction of the recombinant protein. *LoVBPO2a* is an intron-less gene. The coding region was amplified from genomic DNA, using the primer set with a *Nde*I site on the start codon and a *Bam*HI site after the stop codon. The PCR product was digested with *Nde*I and *Bam*HI, excised after agarose gel electrophoresis and ligated into the corresponding sites of pET21a. The expression plasmid, designated as pET-LoVBPO2a, was electroporated into the *E. coli* BL21 (DE3) pLysS (Promega). A 10 ml overnight culture of the transformants was inoculated into 1 l of Luria-Broth medium containing 50 μg ml^{-1} of carbenicillin disodium salt and incubated at 37°C with shaking of 120 rpm until mid-log phase. Overproduction of the recombinant protein was induced by adding IPTG at a final concentration of 0.4 mM. After incubation at 25°C for 3 hours, bacterial cells were harvested by centrifugation at 5000 g for 15 min.

The pellet was suspended into the "basic buffer" defined in this study, consisting of 50 mM Tris-SO_4 (pH 8.0) and 1 mM NH_4VO_3, and disrupted by ultrasonification. After the removal of cell debris by centrifugation at 15000 *g* for 15 min, the supernatant was subjected to 30% ammonium sulphate saturation for precipitation at 4°C overnight. The soluble supernatant was recovered by centrifugation at 9000 *g* for 30 min, dialysed against the basic buffer and applied to the DE52 anion exchange chromatography (GE Healthcare, Chicago, Illinois, USA). After washing the column with the basic buffer, stepwise elution with a series of KBr solutions (0.1, 0.2, 0.3, 0.4 and 0.8 M) was performed. The recombinant protein was eluted with 0.4 M KBr. The fraction containing the protein of interest was dialysed against the basic buffer and concentrated by ultrafiltration. The protein concentrations were quantified by the BCA Protein Assay Kit (Thermo Fisher Scientific). The purified protein was stored at 4°C.

Enzyme assay of LoVBPO

Brominating activity was assayed spectrophotometrically by measuring the decrease in absorbance at 290 nm during the bromination of monochlorodimedone (MCD, ε = 19.9 mM/cm) to monobromomonochlorodimedone for 1 min. The standard condition consisted of 50 mM MES-NaOH (pH 6.0), 200 mM KBr, 50 μM MCD and 1 mM H_2O_2. One unit (U) was defined as the amount of enzyme necessary for substrate conversion of 1 μmol MCD per minute at 25°C (Bernhardt, Okino, Winter, Miyanaga, & Moore, 2011). MCD was purchased from the company (Alfa Aesar, Ward Hill, MA). The pH dependency was tested by changing the pH of the reaction buffer from 4.0 to 6.0 with 50 mM MES-NaOH, and pH was adjusted from 7.0 to 9.0 with 50 mM Tris-HCl. Thermal stability was estimated by the standard assay after treating the enzyme solution for 20 min at different temperatures. Tolerance for polar organic solvents was evaluated by adding 40% (v/v) ethyl alcohol (EtOH), methyl alcohol (MeOH), 2-propanol (2-PrOH), acetonitrile (MeCN) or acetone (ACE). Steady-state kinetic experiments were performed at pH 6.0 or pH 7.0 by changing the concentrations of one substrate while fixing the concentration of another substrate at the saturating level (200 mM for KBr and 1 mM for H_2O_2). The Km values were derived from non-linear fitting to initial data using the GraphPad Prism software (GraphPad Software, San Diego, California, USA).

The activity of LoVBPO2a was also examined with nerolidol according to the published method with some modifications (Carter-Franklin & Butler, 2004). Briefly, 10 mM mixture of *cis*- and *trans*-nerolidol (Tokyo Kasei Kogyo, Tokyo, Japan) was prepared in DMSO. The 50 μl reaction mix was composed of 50 mM MES-NaOH (pH 6.0), 5 mM KBr, 1 mM H_2O_2, 20% (v/v) EtOH and 0.5 mM nerolidol. The reaction was started by adding approximately 1.0 μg of LoVBPO2a and incubated at 25°C for 18 hours under dark conditions. After quenching by adding 200 μl of MeOH, the reaction was mixed with both 1 ml of EtOAc and water and partitioned between them. The EtOAc layer was dried, dissolved in MeOH and desalted using the SPE cartridge Strata C18-E (Phenomenex, Torrance, California, USA). The eluates with 100% MeOH were applied to LC-MS analysis. Mass spectra were collected using Accela-LC and LTQ Orbitrap Discovery (Thermo Fisher Scientific) on a FT-ESI positive

mode. YMC Pack Pro C18 (2.0 × 150 mm) (YMC) was used for the analytical column. The elution program was set a linear gradient of 50–100% MeCN in water containing 0.1% formic acid for 15 min, followed by an isocratic of 100% MeCN for 10 min at a flow rate of 200 μl min^{-1}.

Results

Cloning of the genes for LoVBPO

The sequences of V-BPOs have been established in several red algae, including *Corallina pilulifera* (Shimonishi et al., 1998), *Porphyra yezoensis* (Nikaido et al., 2000) and *L. nipponica* (Kaneko et al., 2014). We collected *in silico* the nucleotide sequences of algal V-BPOs and designed several sets of PCR primers (Supplementary table S1). The organization of the genes for V-BPO was examined by PCR amplification. After sequencing the genome and the inverse PCR products, the full open reading frames were arranged into four distinct members encoding for similar V-BPO-like proteins. All the protein members consist of a peptide of 643 amino acids and share high sequence identities ranging from 98.3% to 100%. Given the similarities with previously reported LnVBPO1 and LnVBPO2 in *L. nipponica* (Kaneko et al., 2014), the four obtained from *L. okamurae* were designated as LoVBPO1a, LoVBPO1b, LoVBPO2a and LoVBPO2b, respectively.

The X-ray crystal structures of V-BPOs from the brown alga *Ascophyllum nodosum* (AnVBPO) (Weyand et al., 1999) and the red alga *Corallina officinalis* (CoVBPO) (Isupov et al., 2000) have been determined. The relationships between protein structure and function of V-BPOs are well understood (Agarwal et al., 2017; Wever et al., 2018). The amino acid sequences of LoVBPOs were aligned with those of the other red algal V-BPOs (Fig 2). The alignment displayed high similarities throughout

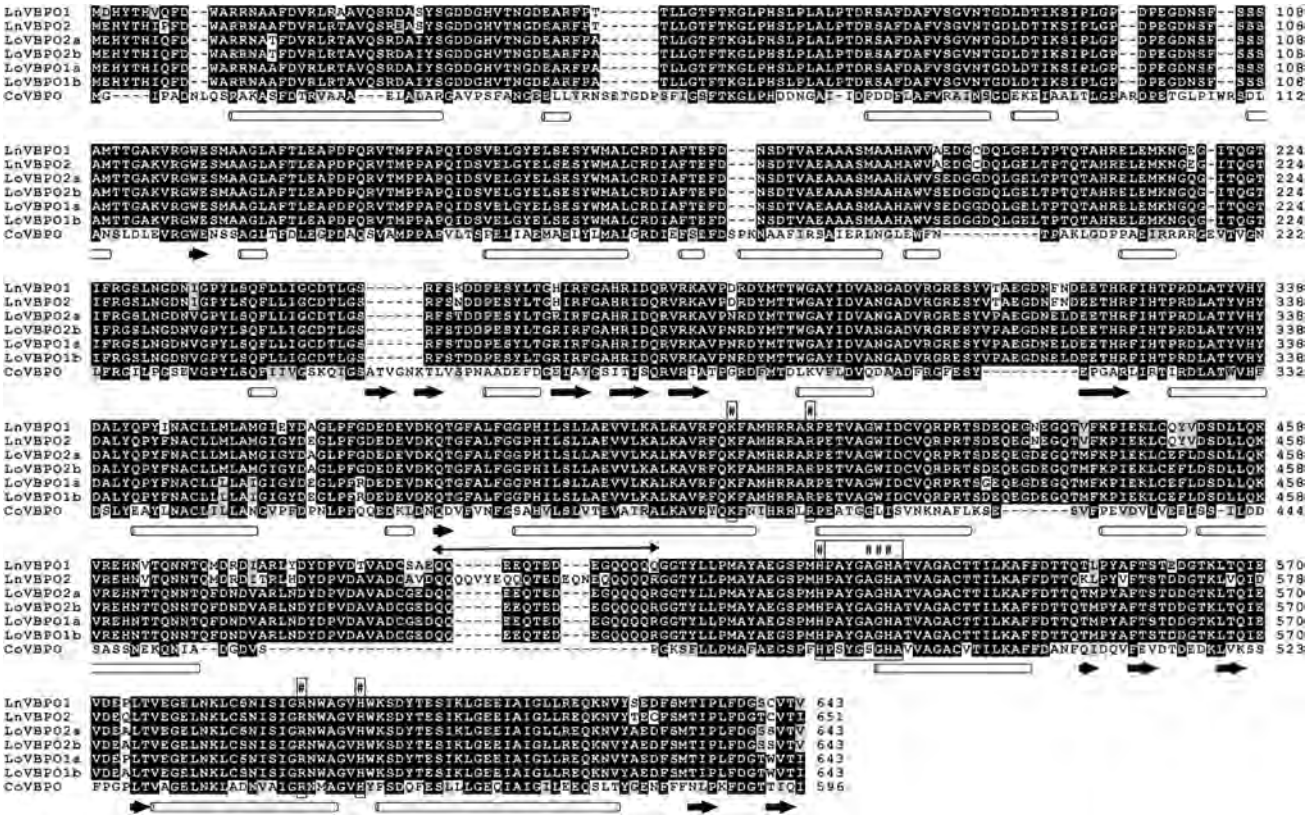

Figure 2. Amino acid alignment of the red algal vanadium-dependent bromoperoxidases. Conserved and biochemically similar amino acids (aa) at each position are indicated by black and grey backgrounds, respectively. The aa responsible for the active centre are boxed and marked by the hash signs. The glutamine-rich repeat region is shown by the double directional arrow. The secondary structures reported in CoVBPO (Isupov et al., 2000) are shown by the open bar (α-helix) and the closed arrow (β-strand), respectively. The database accession numbers in *Corallina officinalis* are: CoVBPO (AAM46061); in *Laurencia nipponica* LnVBPO1 (BAP16518) and LnVBPO2 (BAU59342).

the coding regions, although several gaps or insertions occurred between *Laurencia* and *Corallina*. For instance, the overall identity of LoVBPO2a with LnVBPO1, LnVBPO2 and CoVBPO was 94.1%, 91.7% and 40.5%, respectively.

By analogy with AnVBPO, the vanadium-binding site of CoVBPO is assumed to lie at the core of the four-α-helix bundle, where the vanadium ion covalently binds to the side chain of a conserved His[551] residue, formed by hydrogen bond networks with

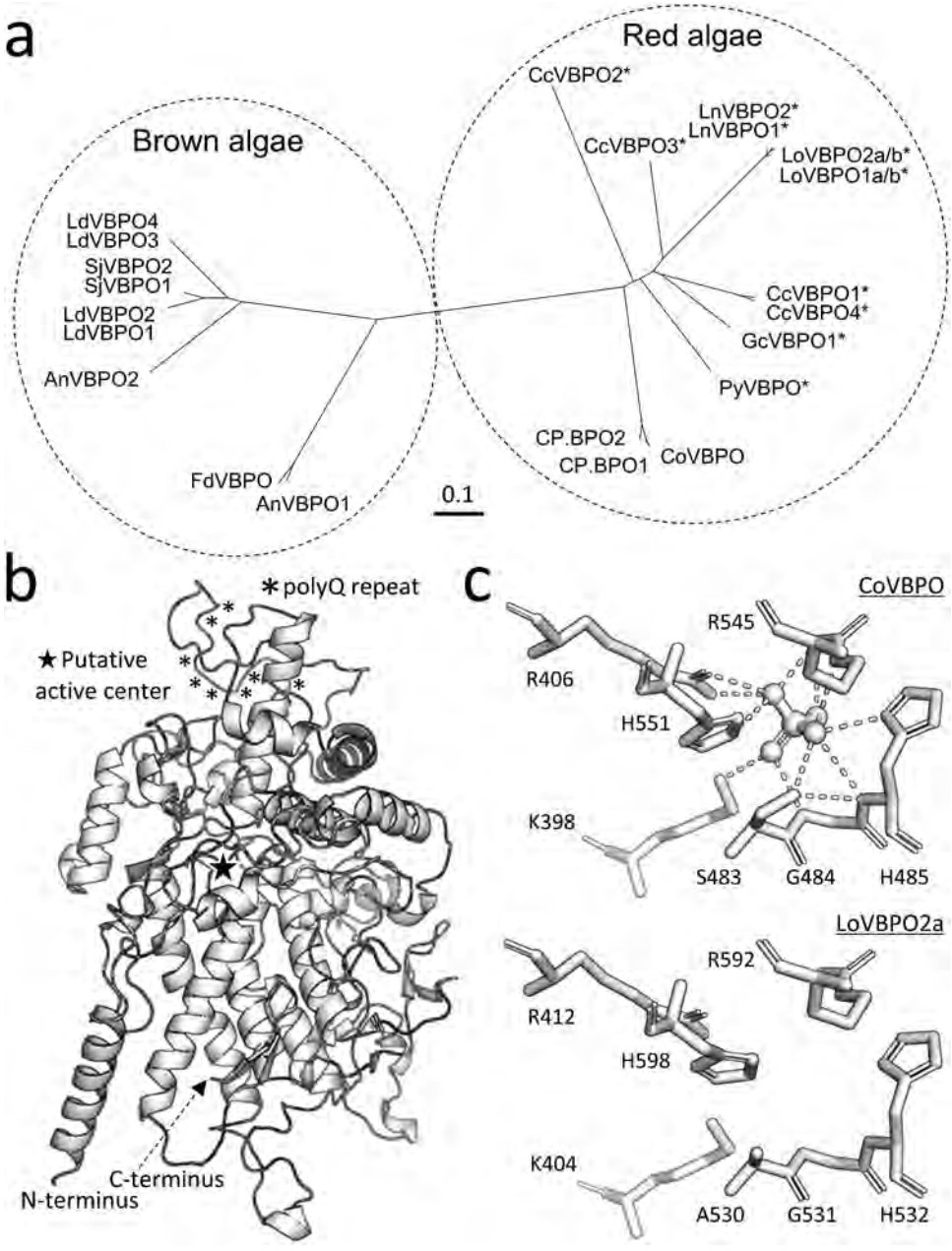

Figure 3. Phylogeny and protein structure of LoVBPO2a. (a) Phylogeny of the vanadium-dependent bromoperoxidases among the marine algae. The phylogenetic tree was constructed by the neighbour-joining method with 1000 bootstrap replications. The protein accession numbers are AnVBPO1–2 (P81701, CCD42013), FdVBPO (AAC35279), LdVBPO1–4 (CAD37191, CAD37192, CAQ51441 and CAQ51442) and SjVBPO1–2 (AYP65252) for the brown algae; CcVBPO1–4 (CDF34418, CDF34463, CDF37939, and CDF40600), CoVBPO (AAM46061), CP.BPO1–2 (BAA31261, BAA31262), GcVBPO1 (AGE00855), LnVBPO1–2 (BAP16518, BAU59342) and PyVBPO (BAQ02347) for the red algae. The V-BPOs carrying the Ala-type active centre are indicated by the asterisks. The scale bar indicates number of amino acid changes per site. (b) Tertiary structure of LoVBPO2a. The monomeric form of LoVBPO2a was predicted by Swiss-PROT. The putative active site is indicated by the star. The asterisks indicate the glutamine-rich repeat region. The N- and C-terminal sites are indicated. (c) Comparison of the vanadate-binding site between CoVBPO and LoVBPO2a. The ligand-binding sites are magnified. The positions of the essential amino acids are indicated. The hydrogen bond networks are displayed by the dotted lines. The vanadate ion is experimentally substituted by the phosphate ion in the crystallized model of CoVBPO.

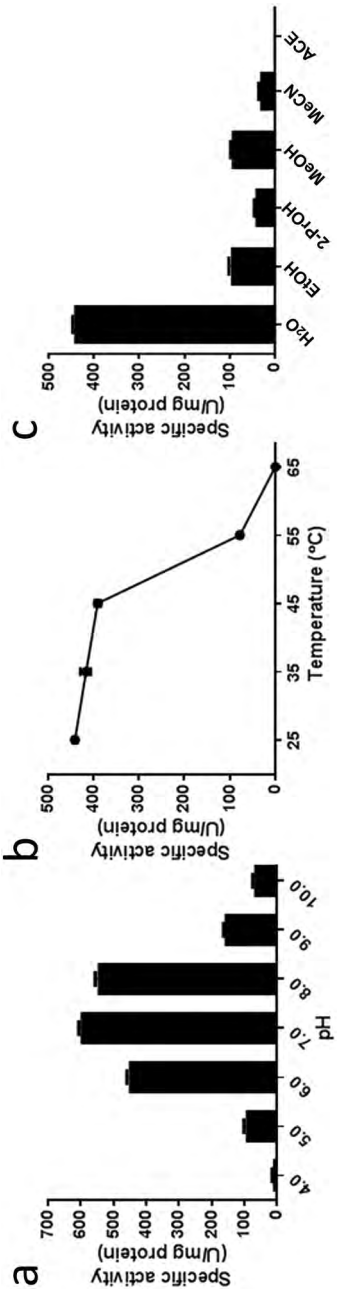

Figure 4. Enzymatic characterization of LoVBPO2a. (a) pH dependency of LoVBPO2a. The MCD assay was conducted under different pH conditions. (b) Thermal stability of LoVBPO2a. The enzyme solution was treated for 20 min at different temperatures and subjected to the MCD assay. (c) Tolerance of organic solvents. A polar organic solvent, including one of ethyl alcohol (EtOH), methyl alcohol (MeOH), 2-propanol (2-PrOH), acetonitrile (MeCN) and acetone (ACE), was added to the reaction at 40% (v/v) and assayed.

the other residues, which makes a protonation pocket for Br^- (Isupov et al., 2000). In addition, an extra His residue proximal to the vanadate-binding site appears to play a supportive role as a proton donor during the oxidation process (Carter, Beatty, Simpson, & Butler, 2002). Sequence comparison with CoVBPO revealed that a set of amino acids responsible for the binding pocket of vanadate were almost completely conserved, except that a Ser^{483} residue in CoVBPO was substituted by an Ala in both LoVBPOs and LnVBPOs. When the amino acid sequences of the algal V-BPOs are compared, there are conserved insertions in the middle C-terminal regions of the V-BPOs of *Laurencia*. It is noteworthy that the insertion sequences contain glutamine-rich repeats (Fig 2, Supplementary fig. S2).

Phylogeny and protein structure of LoVBPO

To infer the lineage origin of LoVBPOs, phylogenetic analysis of the amino acid sequences was performed with the major marine algal V-BPOs (Fig 3a). The phylogenetic tree indicated that the red algal V-BPOs constituted a monophyletic clade and were distinct from the brown algal V-BPOs. Within the red algal clade, early and independent branching of the ancestral genes should give rise to a distinct member of V-BPO. More recent evolutionary events, including gene duplication and diversification of the subfamily, were observed among the V-BPOs of *Laurencia*.

Given the high sequence similarities among the LoVBPOs, LoVBPO2a was chosen for the following experiments. The tertiary structure of LoVBPO2a was predicted by the homology-based SWISS-MODEL using the crystallized structure of CoVBPO (Isupov et al., 2000) as a template (Fig 3b). The monomeric form of LoVBPO2a showed that the core structure mostly consisted of α-helices coordinated with 2 four-α-helix bundles of approximately 180° rotation. It is the common structure motif shared by the majority of V-BPOs (Agarwal et al., 2017). The possible vanadate-binding site of LoVBPO2a was located at the end of a four-α-helix cluster in the C-terminal region. When the predicted structure around the vanadate-binding site of LoVBPO2a was magnified and compared with that of CoVBPO, the amino acid residues involved in binding to vanadate could be superimposed (Fig 3c).

The result showed that the stereochemistry of LoVBPO2a was equivalent to that of CoVBPO; however, a polar Ser^{483} residue carrying a hydroxyl

group in CoVBPO was unusually substituted by a non-polar Ala[530] in LoVBPO2a. The extra glutamine-rich repeat is another feature of the V-BPOs from *Laurencia*. The simulation model showed that the glutamine-rich repeat of LoVBPO2a protruded from a cluster of α-helices and resulted in a bulky structure on the surface of the protein molecule (Fig 3b).

Enzymatic characterization of LoVBPO2a

The recombinant protein of LoVBPO2a was overproduced in *E. coli* and purified with an anion exchange column (Supplementary fig. S1). The brominating activity of LoVBPO2a was examined by assay with monochlorodimedone (MCD), which has been widely used as the universal substrate for halogenating enzymes (Fig 4).

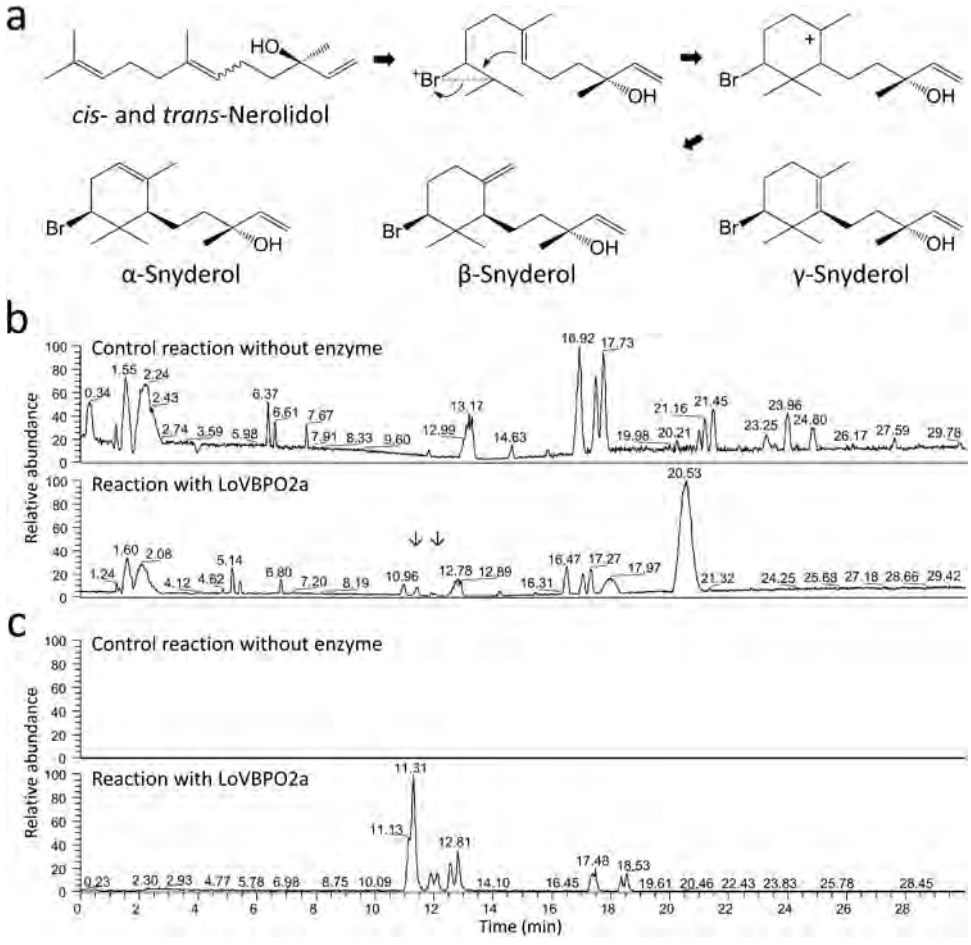

Figure 5. Brominating assay of LoVBPO2a. (a) Proposed synthesis of snyderol isomers from nerolidol. The proposed mechanism is that V-BPO is involved in the asymmetric bromination that triggers the cyclization of a linear precursor, and the cationic intermediate generated by the oxidation of bromide should attack the electron-rich olefinic bond and form three double bonds resulting in closure of a carbon ring. (b) Total ion current of the reaction products with or without LoVBPO2a. The large peaks at 17.97 and 20.53 min with LoVBPO2a are the electrolyte carry-overs in the enzyme solution. Major peaks of the reaction products are indicated by the arrows. (c) Scanning of the m/z targeted snyderol. Several peaks are specifically detected in the reaction with LoVBPO2a.

Table 1. Enzymatic characterization of the red algal vanadium-dependent bromoperoxidases.

Algal species	Recombinant protein	Optimum pH	Km for H_2O_2 (mM)	Km for Br (mM)	Reference
Corallina officinalis	rCVBPO	6.5	0.017	1.2	Carter et al., 2002
Corallina pilulifera	CP.BPO1	6.5	0.1	8.4	Ohshiro et al., 2004
Gracilaria changii	GcVBPO1	7.0	0.71	4.69	Baharuma et al., 2013
Laurencia nipponica	LnVBPO1	7.0	0.026[a]	0.53[a]	Kaneko et al., 2014
	LnVBPO2	7.0	0.025[a]	0.35[a]	
Laurencia okamurae	LoVBPO2a	7.0	0.027[a]	0.29[a]	This study
			0.014[b]	1.38[b]	

[a]Km values at pH 6.0, b; Km values at pH 7.0.

pH dependency was tested over a pH range from 4.0 to 10.0 (Fig 4a). The standard assay accounted for the brominating activity of 477 U mg^{-1} protein at pH 6.0 and 25°C. The activity was maximum at pH 7.0 (640 U mg^{-1} protein) and declined slightly at pH 8.0, with a sharp drop in activity above pH 9.0. The optimum pH of LoVBPO2a was denoted as around pH 7.0.

Previous studies showed that the algal V-BPOs are thermostable and tolerant of organic solvents (Wever et al., 2018). For instance, AnVBPO was active after treatment at 75°C for 20 min and highly tolerant of organic solvents such as EtOH, MeOH and ACE at 80% (v/v) (Tromp, Olafsson, Krenn, & Wever, 1990). The thermal stability of LoVBPO2a was examined at different temperatures (Fig 4b). In contrast to AnVBPO, the activity of LoVBPOs was gradually decreased by heat treatments at 35°C and 45°C for 20 min. Then, it declined sharply with temperatures over 55°C and was completely lost at 65°C. When an organic solvent, including any of EtOH, 2-PrOH, MeOH, MeCN or ACE, was added to the reaction at a 40% (v/v), the activity of LoVBPO2a was significantly decreased or completely abolished by the further addition of ACE (Fig 4c). The results showed that the tolerance of LoVBPO2a to heat treatments and organic solvents was lower than those of the other V-BPOs.

To characterize the properties of LoVBPO2a, steady-state kinetic analysis was performed using KBr and H_2O_2 as the focused co-substrates (Supplementary fig. S3). The MCD assay was conducted at pH 6.0. A Lineweaver–Burk plot demonstrated that the Km for H_2O_2 and Br of LoVBPO2a

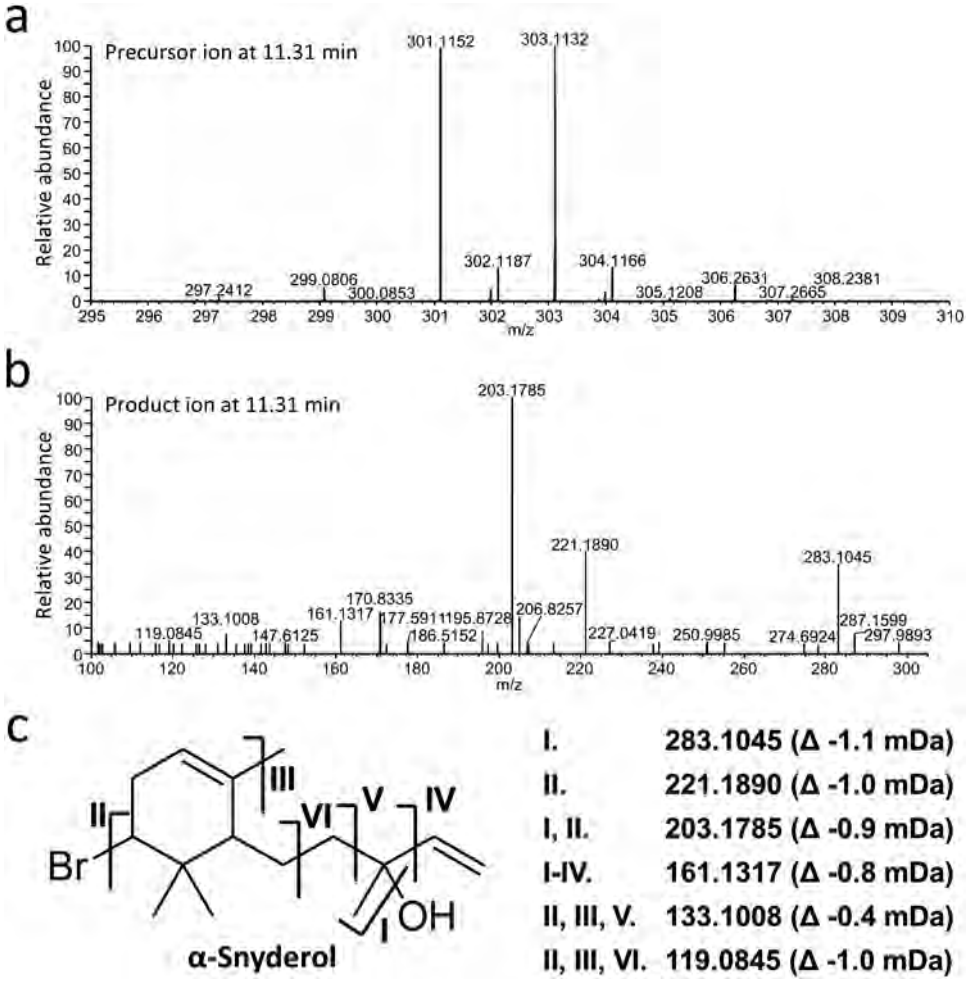

Figure 6. LC-MS detection of the products obtained by the LoVBPO2a-catalysed reaction. (a) Precursor ion detected from the peak at 11.31 min in Fig 5c. A typical signal of monobrominated product is observed. The m/z is similar to that of a $[M + H]^+$ form of snyderol (301.1167 and 303.1147). (b) Product ion derived from the major product synthesized by LoVBPO2a. The MS/MS fragment pattern obtained from the peak at 11.31 min matches that of α-snyderol. (c) Chemical formula and calculated fragment pattern of α-snyderol. The predicted fragmentation patterns and their mass of α-snyderol are denoted. The Δ symbol indicates the difference between the observed and the calculated exact mass.

was 0.027 mM and 0.29 mM, and the kcat (s^{-1}) for H_2O_2 and Br was calculated as 570 and 1419, respectively. The reaction of V-BPO is known to be influenced by pH conditions (De Boer & Wever, 1988). When the same experiment was performed at pH 7.0, the values changed to Km^{H2O2} = 0.014 mM, Km^{Br} = 1.38 mM, $kcat^{H2O2}$ = 964 and $kcat^{Br}$ = 1,583 (Table 1).

Brominating activity of LoVBPO2a

Carter-Franklin & Butler (2004) have reported *in vitro* synthesis of brominated products using (6*E*)-(+)-nerolidol. The reaction with nerolidol and the native V-BPOs purified from the red algae resulted in the synthesis of brominated sesquiterpenes, including a naturally occurring snyderol. Based on this report, a commercially available mixture of *cis*- and *trans*-nerolidol was used for a relevant natural substrate (Fig 5). In the control reaction without LoVBPO2a, the starting materials were detected at 17.45 and 17.73 min due to a mixture of *cis*- and *trans*-nerolidol (Fig 5b). By comparison with the control reaction, minor peaks appeared between 10.96 and 12.78 min. Scanning of the m/z targeted snyderol suggested that multiple products were synthesized by the catalysis of LoVBPO2a, accounting for 8.3% of the conversion rate (Fig 5c).

Analysis of the precursor ions confirmed that all the reaction products consisted of twin signals at ca. m/z 301.1154 and 303.1134 (Fig 6a, Supplementary Fig S4). This is evidence of monobrominated products sharing similar scaffold structures because of the two natural isotopes ^{79}Br and ^{81}Br occurring in a 1:1 ratio. Pioneering work by Carter-Franklin & Butler (2004) clarified the production of olefinic isomers of snyderol during the reaction with nerolidol (Fig 5a). The product ions extracted from the major peak at 11.31 min exhibited a fragment pattern matched to that of α-snyderol, and the intense fragment peak at an m/z 203.1785 was notable in the EI-MS spectrum of 6-*epi*-β-snyderol (Ioannou, Nappo, Avila, Vagias, & Roussis, 2009) (Figs 6b, 6c). Although the reaction products were complicated due to the usage of a mixture of *cis*- and *trans*-nerolidol, the bioorthogonal assay suggested that LoVBPO2a is capable of synthesizing various brominated compounds from nerolidol.

Discussion

V-BPO is one of the key enzymes capable of synthesizing a wide array of sesquiterpenoids (Wever et al., 2018). The synthesis of brominated sesquiterpene is postulated to proceed by the bromonium ion-induced cyclization of a linear precursor (Agarwal et al., 2017). The bromonium ion not only contributes to the cyclization reaction but also is involved in the generation of distinct isomers from a single precursor. The study of red algal V-BPOs confirmed that the olefinic isomers, including α-, β-, and γ-snyderol, were proliferated by *in vitro* reaction with a (6*E*)-(+)-nerolidol (Carter-Franklin & Butler, 2004). α- and β-snyderol are the natural products (Howard & Fenical, 1976). γ-snyderol was not identified from any organisms, while a possible route to a chamigrene skeleton through a γ-snyderol analogue has been hypothesized (Carter-Franklin & Butler, 2004). In this study, the assay of LoVBPO2a showed the occurrence of putative isomers of snyderol from a mixture of *cis*- and *trans*-nerolidol. Comparative analysis of the reaction products has not been completed, but the prolific production of brominated compounds from a single precursor is conserved among the red algal V-BPOs.

The properties of LoVBPO2a discriminated it from the other algal V-BPOs in the MCD assay. Although the tolerance of the enzyme to high temperatures and organic solvents was not high, the Km^{Br} value was markedly low. Previous studies reported Km^{Br} values estimated from the recombinant protein of red algal V-BPOs, from *Corallina officinalis* (Km^{Br} = 1.2 mM at pH = 6.5) (Carter et al., 2002), *C. pilulifera* (8.4 mM at 6.5) (Ohshiro et al., 2004) and *Gracilaria changii* (4.69 mM at 7.0) (Baharuma et al., 2013). These values are high compared with those of LoVBPO2a (0.29 mM at 6.0) as well as LnVBPO1 (0.53 mM at 6.0) and LnVBPO2 (0.35 mM at 6.0) in *L. nipponica* (Kaneko et al., 2014), even though the different pH conditions were taken into consideration. The significantly lower Km^{Br} value is the most striking point shared among the V-BPOs of *Laurencia* (Table 1).

The vanadate-binding pocket of V-BPO is crucial for the oxidative reaction of bromine. Higher tolerances of V-BPO against stressful conditions are thought to be achieved by the rigid active centre (Wever et al., 2018). Previous studies of algal V-BPOs have proposed the importance of the consensus motif P[S/A]YPSGHA, where the vanadate ion is stabilized by hydrogen bond networks

(Isupov et al., 2000). The consensus motif of the red algal V-BPOs is arranged as P[S/A]YG[S/A]GHA. The Ser necessary for a strong hydrogen bond is solely changed to an Ala (Supplementary fig. S2). Because a strong hydrogen bond is lacking, we propose that the structure of the active centre is flexible so that LoVBPO2a is susceptible to the assay conditions (Fig 4). The exchange of amino acids in the active centre was shown to modulate the function of halogenating enzymes, e.g. vanadate binding (Renirie, Hemrika, & Wever, 2000), pH dependency (Carter et al., 2002) and halide specificity (Ohshiro et al., 2004). The genus *Laurencia* produces a diversity of brominated compounds (Wang, Gloer, Ji, & Zhao, 2013). The structure of the active centre may be configured to use bromine in the V-BPOs of *Laurencia*.

The composition of V-BPO members is similar between *L. okamurae* and *L. nipponica* and did not provide clear evidence of diverse production of brominated compounds. However, the differing extent of the glutamine-rich (polyQ) repeat should be mentioned (Fig 2). These polyQ repeats are seldom observed among eukaryotic proteins, mainly in transcription factors (Perutz, 1999).

The roles of the polyQ repeat have been investigated in living cells. Neurodegenerative disorders, such as Kennedy's and Huntington's diseases, result from the expansion of a CAG repeat in the causative genes, which forms extra polyQ repeats in the encoded proteins (Perutz, 1999). An atomic model showed that the polyQ repeat served as the β-strand turn and facilitated the protein–protein association by a polar zipper-like structure, by which longer polyQ repeats tend to be aggregated and become toxic to the cells (Stott, Blackburn, Butler, & Perutz, 1995).

This structure model showed that the polyQ repeat is located on the surface of LoVBPO2a (Fig 3b). Higher-order structures of V-BPOs vary among organismal groups, and the stability of V-BPOs is likely to depend on the cohesiveness of subunits (Butler & Carter-Franklin, 2004). Brown algal as well as *Corallina* V-BPOs appear to be stabilized by the rigid Ser-type active centre (Isupov et al., 2000; Weyand et al., 1999). The Ser necessary for a strong hydrogen bond is changed to A^{481} in the V–IPO of *Laminaria digitata* (Colin et al., 2005). The missing hydrogen bond is thought to be compensated by the recruitment of another K^{403} or stabilized by intramolecular disulphide bridges. Previous work (Isupov et al., 2000) and our preliminary analyses showed that the red algal V-BPOs are homo-multimeric proteins without disulphide bridges. Thus, the polyQ repeat may play a role in the deep connection of subunits. This idea is supported by our previous observation (Kaneko et al., 2014) that the tolerance against high temperatures and organic solvents of LnVBPO2 was higher than those of the other V-BPOs of *Laurencia*, which have a further expansion of the polyQ repeat (Fig 2). Because the polyQ coding regions in the genome appear to be unstable and subject to rapid changes (Schein, 2019), we propose that the ancient origin of *Laurencia* has permitted the genus to evolve the polyQ repeat and utilize it in order to modify the function of V-BPO.

Cuparane- and laurane-type sesquiterpenoids are the main products of *L. okamurae*. These compounds are hypothesized to be synthesized from a common precursor of (2*Z*,6*E*)-farnesol (González, Aguiar, Martín, & Norte, 1975), where V-BPO appears to involve the incorporation of bromide along with a bromonium ion-induced electrophilic attack to the olefin group. The resultant products, including aplysin (Liu et al., 2014) and laurinterol (García-Davis et al., 2019), are of pharmaceutical significance, and the stable nature of V-BPOs in stressful conditions is expected to have practical value in industrial fields (Wever et al., 2018). The results obtained in this study, namely the atypical structure of the active centre and insertion of the polyQ repeat common in the V-BPOs of *Laurencia*, add to the understanding of the function of V-BPOs and also the unique natural halogen-containing metabolites.

Acknowledgments

We are grateful to Kazusa DNA Research Institute for providing us with the cDNA clones of *Porphyra yezoensis*.

Author contributions

KW, KK and TO conceived and designed the study. TI and XRT performed the analyses and prepared figures and tables. KW, MM and KK co-wrote and revised the manuscript.

Disclosure statement

The authors declare no conflicts of interest associated with this manuscript.

Funding

This work was supported in part by a Grant-in-Aid for Scientific Research (KAKENHI) from the Japan Society for the Promotion of Science (JSPS) to TO (16H04975).

ORCID

Kenji Washio http://orcid.org/0000-0001-9065-1816
Masaaki Morikawa http://orcid.org/0000-0003-1547-8069
Tatsufumi Okino http://orcid.org/0000-0002-8363-0467

References

Abe, T., & Masuda, M. (1998). *Laurencia japonensis* sp. nov. (Ceramiales, Rhodophyta). *European Journal of Phycology*, *33*, 17–24.

Agarwal, V., Miles, Z. D., Winter, J. M., Eustáquio, A. S., Gamal, A. A. E., & Moore, B. S. (2017). Enzymatic halogenation and dehalogenation reactions: Pervasive and mechanistically diverse. *Chemical Reviews*, *117*, 5619–5674.

Baharuma, H., Chu, W. C., Teo, S. S., Ng, K. Y., Rahima, R. A., & Ho, C. L. (2013). Molecular cloning, homology modeling and site-directed mutagenesis of vanadium-dependent bromoperoxidase (GcVBPO1) from *Gracilaria changii* (Rhodophyta). *Phytochemistry*, *92*, 49–59.

Bernhardt, P., Okino, T., Winter, J. M., Miyanaga, A., & Moore, B. S. (2011). A stereoselective vanadium-dependent chloroperoxidase in bacterial antibiotic biosynthesis. *Journal of the American Chemical Society*, *133*, 4268–4270.

Butler, A., & Carter-Franklin, J. N. (2004). The role of vanadium bromoperoxidase in the biosynthesis of halogenated marine natural products. *Natural Product Reports*, *21*, 180–188.

Carter, J. N., Beatty, K. E., Simpson, M. T., & Butler, A. (2002). Reactivity of recombinant and mutant vanadium bromoperoxidase from the red alga *Corallina officinalis*. *Journal of Inorganic Biochemistry*, *91*, 59–69.

Carter-Franklin, J. N., & Butler, A. (2004). Vanadium bromoperoxidase-catalyzed biosynthesis of halogenated marine natural products. *Journal of the American Chemical Society*, *126*, 15060–15066.

Colin, C., Leblanc, C., Michel, G., Wagner, E., Leize-Wagner, E., Van Dorsselaer, A., & Potin, P. (2005). Vanadium-dependent iodoperoxidases in *Laminaria digitata*, a novel biochemical function diverging from brown algal bromoperoxidases. *Journal of Biological Inorganic Chemistry*, *10*, 156–166.

De Boer, E., & Wever, R. (1988). The reaction mechanism of the novel vanadium-bromoperoxidase. *Journal of Biological Chemistry*, *263*, 12326–12332.

Fukuzawa, A., Aye, M., Takasugi, Y., Nakamura, M., Tamura, M., & Murai, A. (1994). Enzymatic bromo-ether cyclization of laurediols with bromoperoxidase. *Chemistry Letters*, *23*, 2307–2310.

García-Davis, S., Viveros-Valdez, E., Díaz-Marrero, A. R., Fernández, J. J., Valencia-Mercado, D., Esquivel-Hernández, O., … Guzmán-Delgado, N. E. (2019). Antitumoral effect of laurinterol on 3D culture of breast cancer explants. *Marine Drugs*, *17*, 201.

González, A. G., Aguiar, J. M., Martín, J. D., & Norte, M. (1975). Three new sesquiterpenoids from the marine alga. *Tetrahedron Letters*, *16*, 2499–2502.

Guiry, M. D., & Guiry, G. M. (2022). *AlgaeBase*. Galway: World-wide electronic publication, National University of Ireland. http://www.algaebase.org

Harizani, M., Ioannou, E., & Roussis, V. (2016). The *Laurencia* paradox: An endless source of chemodiversity. *Progress in the Chemistry of Organic Natural Products*, *102*, 91–252.

Howard, B. M., & Fenical, W. (1976). α- and β-snyderol; new bromo-monocyclic sesquiterpenes from the seaweed *Laurencia*. *Tetrahedron Letters*, *17*, 41–44.

Ioannou, E., Nappo, M., Avila, C., Vagias, C., & Roussis, V. (2009). Metabolites from the sea hare *Aplysia fasciata*. *Journal of Natural Products*, *72*, 1716–1719.

Ishihara, J., Kanoh, N., & Murai, A. (1995). Enzymatic reaction of (3*E*,6*S*,7*S*)-laurediol and the molecular modeling studies on the cyclization of laurediols. *Tetrahedron Letters*, *36*, 737–740.

Isupov, M. N., Dalby, A. R., Brindley, A. A., Izumi, Y., Tanabe, T., Murshudov, G. N., & Littlechild, J. A. (2000). Crystal structure of dodecameric vanadium-dependent bromoperoxidase from the red algae *Corallina officinalis* 1 1Edited by R. Huber. *Journal of Molecular Biology*, *299*, 1035–1049.

Kaneko, K., Washio, K., Umezawa, T., Matsuda, F., Morikawa, M., & Okino, T. (2014). cDNA cloning and characterization of vanadium-dependent bromoperoxidases from the red alga *Laurencia nipponica*. *Bioscience, Biotechnology, and Biochemistry*, *78*, 1310–1319.

Katoh, K., Rozewicki, J., & Yamada, K. D. (2019). MAFFT online service: Multiple sequence alignment, interactive sequence choice and visualization. *Briefings in Bioinformatics*, *20*, 1160–1166.

Kersten, R. D., Lee, S., Fujita, D., Pluskal, T., Kram, S., Smith, J. E., … Weng, J. K. (2017). A red algal bourbonane sesquiterpene synthase defined by microgram-scale NMR-coupled crystalline sponge X-ray diffraction analysis. *Journal of the American Chemical Society*, *139*, 16838–16844.

Kuraku, S., Zmasek, C. M., Nishimura, O., & Katoh, K. (2013). aLeaves facilitates on-demand exploration of metazoan gene family trees on MAFFT sequence alignment server with enhanced interactivity. *Nucleic Acids Research*, *41*, W22–W28.

Liu, J., Ma, L., Wu, N., Liu, G., Zheng, L., & Lin, X. (2014). Aplysin sensitizes cancer cells to TRAIL by suppressing P38 MAPK/survivin pathway. *Marine Drugs*, *12*, 5072–5088.

Masuda, M., Abe, T., Suzuki, T., & Suzuki, M. (1996). Morphological and chemotaxonomic studies on *Laurencia composita* and *L. okamurae* (Ceramiales, Rhodophyta). *Phycologia*, *35*, 550–562.

Nikaido, I., Asamizu, E., Nakajima, M., Nakamura, Y., Saga, N., & Tabata, S. (2000). Generation of 10,154 expressed sequence tags from a leafy gametophyte of a marine red alga, *Porphyra yezoensis*. *DNA Research*, *7*, 223–227.

Ohshiro, T., Littlechild, J., Garcia-Rodriguez, E., Isupov, M. N., Iida, Y., Kobayashi, T., & Izumi, Y. (2004). Modification of halogen specificity of a vanadium-dependent bromoperoxidase. *Protein Science*, *13*, 1566–1571.

Perutz, M. F. (1999). Glutamine repeats and neurodegenerative diseases: Molecular aspects. *Trends in Biochemical Sciences*, *24*, 58–63.

Renirie, R., Hemrika, W., & Wever, R. (2000). Peroxidase and phosphatase activity of active-site mutants of vanadium chloroperoxidase from the fungus *Curvularia inaequalis*. Implications for the catalytic mechanisms. *Journal of Biological Chemistry*, *275*, 11650–11657.

Saito, Y. (1989). Conspecificity of two Japanese *Laurencia* species: *L. okamurae* and *L. japonica*. *Japanese Journal of Phycology*, *37*, 208–212.

Sambrook, J., & Russell, D. W. (2001). *Molecular cloning: A laboratory manual* (3rd ed.). Cold Spring Harbor, NY: Cold Spring Harbor Laboratory Press.

Schein, C. H. (2019). Polyglutamine repeats in viruses. *Molecular Neurobiology*, *56*, 3664–3675.

Shimonishi, M., Kuwamoto, S., Inoue, H., Wever, R., Ohshiro, T., Izumi, Y., & Tanabe, T. (1998). Cloning and expression of the gene for a vanadium-dependent bromoperoxidase from a marine macro-alga, *Corallina pilulifera* 1. *FEBS Letters*, *428*, 105–110.

Stott, K., Blackburn, J. M., Butler, P. J., & Perutz, M. (1995). Incorporation of glutamine repeats makes protein oligomerize: Implications for neurodegenerative diseases. *Proceedings of the National Academy of Sciences of the United States of America*, *92*, 6509–6513.

Tromp, M. G., Olafsson, G., Krenn, B. E., & Wever, R. (1990). Some structural aspects of vanadium bromoperoxidase from *Ascophyllum nodosum*. *Biochimica Et Biophysica Acta*, *1040*, 192–198.

Wang, B. G., Gloer, J. B., Ji, N. Y., & Zhao, J. C. (2013). Halogenated organic molecules of rhodomelaceae origin: Chemistry and biology. *Chemical Reviews*, *113*, 3632–3685.

Wever, R., Krenn, B. E., & Renirie, R. (2018). Marine vanadium-dependent haloperoxidases, their isolation, characterization, and application. *Methods in Enzymology*, *605*, 141–201.

Weyand, M., Hecht, H., Kiess, M., Liaud, M., Vilter, H., & Schomburg, D. (1999). X-ray structure determination of a vanadium-dependent haloperoxidase from *Ascophyllum nodosum* at 2.0 Å resolution 1 1Edited by R. Huber. *Journal of Molecular Biology*, *293*, 595–611.